TÜBİTAK

Turkish Journal of Chemistry

http://journals.tubitak.gov.tr/chem/

Research Article

Turk J Chem
(2016) 40: 576 – 587

doi:10.3906/kim-1507-95

CO_2 adsorption behavior and kinetics on chemically modified activated carbons

Burcu Selen ÇAĞLAYAN[1,2], **Ahmet Erhan AKSOYLU**[1,*]
[1]Department of Chemical Engineering, Boğaziçi University, İstanbul, Turkey
[2]Advanced Technologies R&D Center, Boğaziçi University, İstanbul, Turkey

Received: 31.07.2015 • **Accepted/Published Online:** 13.12.2015 • **Final Version:** 21.06.2016

Abstract: CO_2 adsorption capacities of activated carbon-based adsorbents subjected to different treatments, such as HNO_3 oxidation, air oxidation, alkali impregnation, and heat treatment under helium gas atmosphere, were determined by gravimetric analyses and reported previously by our group. In the current work, the experimental adsorption isotherms of these modified activated carbon samples were fitted to Langmuir, Freundlich, and Dubinin–Radushkevich (D-R) models. The best fits were obtained to the D-R equation, indicating competitive or multilayer CO_2 adsorption occurring in the micropores of the adsorbents. Air oxidation followed by alkali impregnation led to the highest micropore volume, ranging between 0.259 and 0.298 g.CO_2/g.adsorbent, which resulted in the highest CO_2 adsorption capacity of 8.87% at 1 atm and 25 °C. The CO_2 adsorption kinetic plots revealed a two-step adsorption process for all the adsorbents: a relatively fast kinetic region phase followed by a slow one until reaching the equilibrium. Pseudo-first and pseudo-second order kinetics explain adsorption for the kinetic region for most of the samples. When the whole adsorption data range is considered, the adsorption cannot be explained by any model at 25 °C due to the complex nature of the adsorbents, but the adsorption behavior fits rather well to pseudo-first order kinetics at 120 °C for the alkali-impregnated samples.

Key words: Activated carbon adsorbents, adsorption kinetics, activated carbon modification, CO_2 adsorption isotherms

1. Introduction

According to the International Energy Agency (IEA), fossil fuels account for more than 80% of present world energy consumption. Additionally, the growing economies of developing nations are expected to require significantly more energy to meet expected future demand, much of which could come from fossil fuels. Carbon capture and storage technologies continue to gain importance due to the rising greenhouse gas emissions, of which CO_2 accounts for ca. 80%, majorly resulting from fossil fuel consumption. Among the CO_2 capture technologies, adsorption stands out from the others with its cost advantage, high efficiency, versatility, and ease of applicability over a relatively wide range of temperatures and pressures.[1–4] Moisture-resistant porous adsorbents with large surface areas such as activated carbons are very suitable for CO_2 adsorption. In addition to their advantageous properties like robustness and their high CO_2 adsorption capacities, the surface chemistry of the activated carbons can be modified by chemical activation to increase the adsorption capacity even further. Oxidative pretreatments,[5,6] heat treatment with ammonia,[7–11] and slurry/solution impregnation are widely used techniques that modify the surface chemistry of the activated carbon.[4,12–16] Researchers have reported improved CO_2 adsorption capacities upon NaOH,[12,13] KOH,[13] Na_2CO_3,[4,13] MgO,[14] CaO,[14,15] $ZnCO_3$,[15] and $Ca(C_2H_3O_2)_2$[16] impregnation for carbon-based adsorbents. Our group has previously designed and tested

*Correspondence: aksoylu@boun.edu.tr

modified (oxidized and Na_2CO_3-impregnated) activated carbon-based adsorbents and reported approximately 15-fold CO_2 adsorption capacity compared to that of their nonimpregnated supports.[4]

The CO_2 adsorption test results obtained may be used to get further information about the material that is studied, as the physical adsorption of gases and vapors is a very useful technique for the characterization of microporous solids.[17] For many years, since the surface area was presumed to be the measure of adsorption capacity, microporous solids such as activated carbons have been characterized using the B.E.T. method applied to the adsorption isotherm.[18] As the surface area is inadequate for giving information about the pore size, pore shape, and pore surface chemistry, over the past 50 years methods of isotherm analysis have been used to get an overview of the pore structure.[18,19] The choice of the appropriate equation for parameter evaluation that characterizes the microporous structure is crucial. Among the many theoretical or empirical adsorption isotherm equations, the Freundlich and Langmuir equations are the ones used most often.[20] The simplest theoretical model that can be used to describe monolayer adsorption is the Langmuir equation, which assumes a uniform surface, a single layer of adsorbed material, and constant temperature.[21,22] The Langmuir equation may be written as follows:

$$\frac{P}{Q} = \frac{1}{Q_m}P + \frac{1}{bQ_m},$$

where Q is the amount adsorbed (mmol/g adsorbent), P is the pressure (mmHg), Q_m is the theoretical monolayer saturation capacity, and b is the Langmuir isotherm constant. Thus the plot of P/Q against P should be linear with a slope and intercept of $1/Q_m$ and $1/bQ_m$, respectively. This model is useful when there is a strong specific interaction between the surface and the adsorbate so that no multilayer adsorption occurs.[20,21]

The Freundlich equation is an empirical formula that provides a very reasonable description of nonlinear adsorption behavior involving heterogeneous surfaces considering adsorption enthalpy change with surface concentration. The equation can be written in the form

$$Q = kP^{1/n},$$

where k and n are Freundlich constants representing adsorption capacity and adsorption intensity, respectively.[20,23] A plot of log(Q) versus log(P) gives the values of k and n.

Since competitive or multilayer adsorption can occur on microporous adsorbents, one may choose to use the popular equation proposed by Dubinin and Radushkevich, which describes the adsorption of gases and vapors on microporous adsorbents such as carbons.[17,22,24,25] The Dubinin–Radushkevich (D-R) equation may be written as

$$\frac{W}{W_0} = exp\left[-\left(\frac{RT}{E}ln\left(\frac{P}{P_0}\right)\right)^2\right],$$

where W is the amount of gas adsorbed per unit mass of adsorbent (g/g catalyst), W_0 is micropore capacity (g/g catalyst), R is the universal gas constant (8.315 J/mol K), T is the temperature (K), E is the characteristic energy (J/mol), and P_0 is the saturation pressure (mmHg). Thus, one can obtain the micropore capacity and characteristic energy by plotting ln(W) versus $(\ln(P/P_0))^2$.

A predictive model using thermodynamic equilibrium and reliable kinetic parameters may provide a method for estimating the adsorption dynamics and CO_2 adsorption column sizing without extensive

experimentation.[26,27] It is possible to fit the kinetic data to both pseudo-first and pseudo-second order models aiming to determine the appropriate reaction order for the adsorption processes based on R^2 correlation coefficient values.[28–32] The linear form of the pseudo-first order kinetic model is given by

$$\ln(q_e - q_t) = \ln q_e - k_1 t,$$

where q_e and q_t are the amount adsorbed in mg/g at equilibrium time and any time t (min), respectively, and k_1 is the pseudo-first order rate constant (min^{-1}). The rate constant can be obtained from the slope of ln ($q_e - q_t$) versus t plot.

The linear form of the pseudo-second order kinetic model can be expressed as

$$\frac{t}{q_t} = \frac{1}{k_2 q_e^2} + \frac{t}{q_e},$$

where k_2 is the pseudo-second order rate constant (mg g^{-1} min^{-1}), and the plot of t/q_t versus t gives the values of k_2 and q_e.

Studies on the kinetics of adsorption on porous adsorbents have put forward different uptake kinetics under similar conditions originating from different facts such as diffusion controlled by surface resistance, internal defects, intraparticle diffusion, and heat transfer.[33,34] The initial rate of intraparticle diffusion can be calculated using

$$q_t = k_{id} t^{0.5} + C,$$

where k_{id} is the intraparticle diffusion rate constant (mg g^{-1} $min^{-0.5}$) and C (mg/g) is a constant that gives an idea about the thickness of the boundary layer.[29,31,34] k_{id} can be obtained from the slope of the q_t versus $t^{0.5}$ plot.

The aim of the current work was to determine the CO_2 adsorption behavior of activated carbon samples subjected to different treatments, such as HNO_3 oxidation, air oxidation, alkali impregnation, and heat treatment, and to obtain information on CO_2 adsorption kinetics on them. In this context, first the experimental adsorption isotherms, which were determined previously for 25, 120/180, and 200 °C temperature levels and 0–20 bar pressure range,[4] were fitted to Langmuir, Freundlich, and D-R models, and the goodness of fit for those models was comparatively analyzed. These studies were followed by the search for the best kinetic model for CO_2 adsorption on those samples for the same temperature levels and 1 bar CO_2 pressure.

2. Results and discussion

The experimental adsorption isotherms were fitted to Langmuir, Freundlich, and D-R models to describe the adsorption characteristics of the designed and prepared adsorbents; a better fit was obtained to the D-R equation with a correlation coefficient of 0.99 (Tables 1–3). The correlation coefficients (R^2) (Tables 1 and 2) indicated that the Langmuir and Freundlich models can also be used to explain the data and to estimate the adsorption parameters for all AC4 and AC5 samples except for AC4-300, which has a correlation coefficient of 0.403 for the Langmuir equation. Figure 1 is given as an example of the Langmuir isotherms for AC4-250 adsorbent. The comparative analysis indicated that between the two models CO_2 adsorption on all AC4 and AC5 samples could be better explained by the Freundlich isotherm. Thus, the possibility of monolayer adsorption (constant heat of adsorption for all sites) on the active homogeneous sites present within the adsorbent, which the Langmuir model is based on,[20,23] is eliminated. Previous EDS and DRIFTS studies conducted on AC4 and AC5 samples

have proven the heterogeneous structure of the active sites on the Na_2CO_3 impregnated samples. The Na sites, which have CO_2 adsorption ability, are highly dispersed on the AC support, yielding enhanced CO_2 adsorption capacity of the AC-based adsorbent. Moreover, free carboxylic acid sites of the AC support, i.e. the carboxylic acid sites that are not coordinated to Na precursor, decompose to CO_2 upon heat treatment, forming uncoordinated C sites that can easily adsorb CO_2; those sites provide additional CO_2 adsorption capacity to the impregnated adsorbent.[4] As expected, CO_2 adsorption isotherms for AC1, AC2, and AC3 samples did not fit the Langmuir or Freundlich models; in addition to the nonoverlapping adsorption and desorption isotherms during cyclic tests, adsorption capacity increases for those samples at elevated temperatures. This can be attributed to the decomposition of the oxygen-bearing surface groups with the rise in temperature. Upon the decomposition of those surface groups, uncoordinated/free C sites are formed, which can readily adsorb CO_2,[4] and this can be considered an indication of chemically activated adsorption.

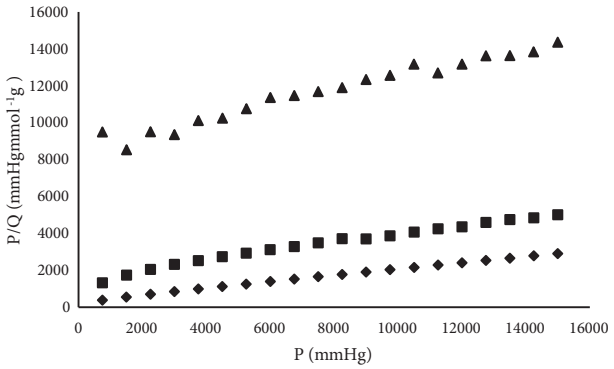

Figure 1. Langmuir isotherms for CO_2 adsorption on AC4-250 at (♦) 25 °C, (■) 120 °C, and (▲) 200 °C.

Table 1. Parameters obtained by Langmuir equation.

Adsorbent	Freundlich constants (25 °C)			Freundlich constants (120/180 °C *)			Freundlich constants (200 °C)		
	Q_m^{**}	b	R^2	Q_m^{**}	b	R^2	Q_m^{**}	b	R^2
AC1	0.955	0.00023	0.993	**6.238**	**0.00001**	**0.118**	1.707	0.00011	0.968
AC2	0.782	0.00022	0.994	**−7.184**	**−0.00001**	**0.327**	2.566	0.00004	0.984
AC3	0.711	0.00015	0.977	**−0.457**	**−0.00003**	**0.527**	2.357	0.00003	0.830
AC4-200	5.123	0.00053	0.999	2.800	0.00014	0.988	1.950	0.00006	0.916
AC4-250	5.731	0.00056	0.999	4.158	0.00016	0.984	2.610	0.00004	0.968
AC4-300	5.216	0.00051	0.991	3.316	0.00016	0.990	1.740	0.00003	0.403
AC5-175	4.286	0.00052	0.997	2.028	0.00015	0.916	0.887	0.00012	0.979
AC5-200	1.520	0.22721	0.978	2.266	0.00022	0.986	1.032	0.00011	0.944
AC5-250	3.449	0.00047	0.996	2.594	0.00022	0.986	1.731	0.00012	0.948
AC5-250-400He	4.701	0.00043	0.995	2.584	0.00019	0.986	1.742	0.00010	0.987
AC4-300-600He	5.216	0.00051	0.991	4.440	0.00007	0.971	2.660	0.00004	0.952

(*) Data collected at 180 °C are shown in bold. (**) Qm is in mmol/g adsorbent.

Table 2 shows the Freundlich equation parameters k and 1/n values at different temperature levels. Figure 2 is given as an example of the log(Q) versus log(P) plots allowing the determination of those parameters. The Freundlich isotherm assumes a heterogeneous surface (multilayer adsorption) with a nonuniform distribution of heat of adsorption over it.[35,36] The decrease in the values of k, which can be interpreted as a measure

Table 2. Parameters obtained by Freundlich equation.

Adsorbent	Freundlich constants (25 °C)			Freundlich constants (120/180 °C *)			Freundlich constants (200 °C)		
	k	1/n	R^2	k	1/n	R^2	k	1/n	R^2
AC1	0.00655	0.5016	0.9872	**0.00000**	**1.6069**	**0.708**	0.00170	0.6785	0.9787
AC2	0.00432	0.5228	0.9864	**0.00004**	**1.0643**	**0.998**	0.00038	0.8282	0.9938
AC3	0.00196	0.5833	0.9959	**0.00000**	**1.4300**	**0.901**	0.00006	1.0076	0.9554
AC4-200	0.26461	0.3023	0.9707	0.00770	0.5816	0.994	0.00063	0.7580	0.9988
AC4-250	0.32509	0.2933	0.9683	0.01551	0.5517	0.997	0.00040	0.8254	0.9931
AC4-300	0.23632	0.3106	0.9717	0.01097	0.5648	0.994	0.00010	0.8990	0.9688
AC5-175	0.26369	0.2827	0.9891	0.00998	0.5203	0.947	0.00139	0.6317	0.9946
AC5-200	0.26014	0.2887	0.9896	0.01951	0.4731	0.995	0.00127	0.6581	0.9783
AC5-250	0.17624	0.3006	0.9926	0.02263	0.4716	0.996	0.00194	0.6705	0.9501
AC5-250-400He	0.20564	0.316	0.9925	0.01703	0.4984	0.997	0.00189	0.6659	0.993
AC4-300-600He	0.05553	0.4799	0.9793	0.00205	0.7462	0.99	0.00094	0.7341	0.9904

(*) Data collected at 180 °C are shown in bold.

Table 3. Parameters obtained by D-R equation.

Adsorbent	D-R constants (25 °C)			D-R constants (120/180 °C*)			D-R constants (200 °C)		
	Wo (g/gcat)	E (kJ/mol)	R^2	Wo (g/gcat)	E (kJ/mol)	R^2	Wo (g/gcat)	E (kJ/mol)	R^2
AC1	0.0498	6.581	0.999	**0.1684**	**4.018**	**0.995**	0.0834	5.517	0.995
AC2	0.0408	6.449	0.998	**0.0959**	**4.433**	**0.994**	0.0871	5.014	0.998
AC3	0.0342	6.129	0.992	**0.0648**	**3.582**	**0.990**	0.0723	4.754	0.994
AC4-200	0.2669	8.250	0.997	0.1381	5.981	0.998	0.0760	5.035	0.990
AC4-250	0.2980	8.376	0.996	0.2035	6.152	0.995	0.0885	5.022	0.997
AC4-300	0.2588	8.142	0.997	0.1654	6.070	0.999	0.0406	4.966	0.988
AC5-175	0.2158	8.569	1.000	0.1258	5.225	0.988	0.0419	5.745	0.995
AC5-200	0.2265	8.478	1.000	0.1139	6.638	0.997	0.0504	5.611	0.992
AC5-250	0.1733	8.315	0.999	0.1300	6.650	0.996	0.0879	5.490	0.976
AC5-250-400He	0.2370	8.112	0.999	0.1290	6.470	0.997	0.0809	5.590	0.998
AC4-300-600He	0.2639	8.278	0.997	0.1614	5.863	0.996	0.0821	5.316	0.994

(*) Data collected at 180 °C are shown in bold.

of adsorption capacity under specified conditions,[20,37] at higher temperatures shows that the adsorption rate decreases with a rise in temperature. For Freundlich isotherms, the 1/n constant is an important parameter of exchange intensity or surface heterogeneity, and it ranges between 0 and 1. As shown in Table 2, the values of 1/n were between 0 and 1 for all the AC4 and AC5 samples, suggesting that the use of the Freundlich isotherm is favorable.[36] It has been shown that high values of 1/n reflect relatively uniform surfaces.[37] Keeping this fact in mind, one can conclude that AC4 and AC5 samples show similar surface characteristics in terms of heterogeneity at room temperature. However, at elevated temperatures, a sharp decrease in the extent of surface heterogeneity for AC4 samples, including the high temperature He-treated one, was observed. A similar decrease is also evident for all the AC5 adsorbents although not as much as that of the AC4 samples. This may be due to the fact that AC5 adsorbents are richer in carboxylic acid and aromatic groups as revealed by the FTIR-DRIFTS studies.[4]

The experimental data plotted in accordance with the D-R adsorption isotherms, having characteristic curves that describe adsorption capacity, are given in Figure 3 for AC4-250 sample as an example. The characteristic energy and the micropore capacity of all the adsorbent samples studied are presented in Table 3. The micropore capacity of the HCl-treated (AC1), air-oxidized (AC2), and HNO_3-oxidized samples (AC3) was observed to increase with temperature, whereas for the air-oxidized Na_2CO_3-impregnated (AC4) and nitric acid-oxidized Na_2CO_3-impregnated (AC5) samples, it was found to decrease as the temperature increased. The highest micropore capacity was obtained for AC4-250 sample at 25 °C (Table 5), which is in accordance

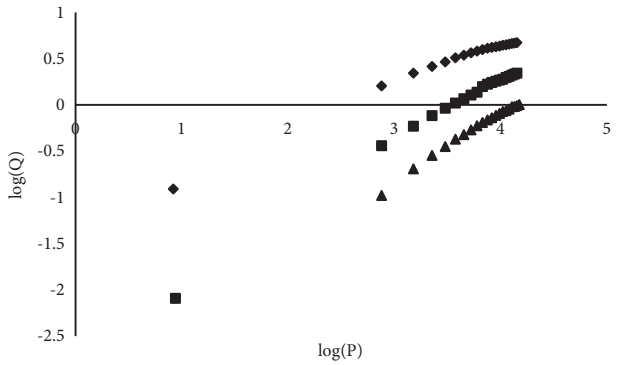

Figure 2. Freundlich isotherms for CO_2 adsorption on AC4-300-600He at (♦) 25 °C, (■) 120 °C, and (▲) 200 °C.

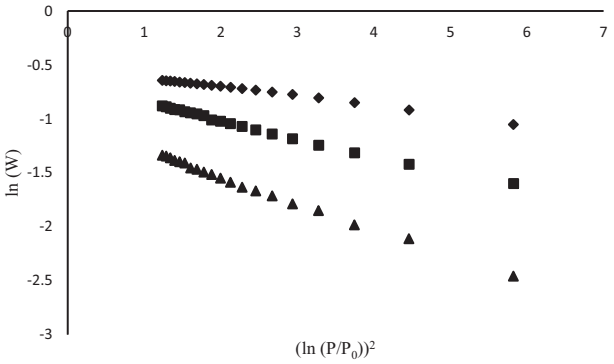

Figure 3. Dubinin–Radushkevich isotherms for CO_2 adsorption on AC4-250 at (♦) 25 °C, (■) 120 °C, and (▲) 200 °C.

with the experimental results (Table 4). The characteristic energies (E) of the alkali-impregnated adsorbents were higher than those of the nonimpregnated samples at 25 °C. However, at 200 °C, no difference between the E values of the alkali impregnated and nonimpregnated ones was observed as the characteristic energies of the AC4 and AC5 samples were found to decrease with increasing temperature. The value of E provides information about the adsorption mechanism. Values below 8 kJ/mol indicate physical adsorption, whereas characteristic energies above that value up to 16 kJ/mol point to ion exchange.[31] Therefore, we can conclude that physisorption is the adsorption mechanism for all the adsorbents studied at all temperature levels and for AC4 and AC5 samples at 25 °C ion exchange mechanism may have played an additional role. Furthermore, for all the activated carbon-based adsorbents studied, the D-R plots consist of only one section, suggesting only one micropore size range is observed in these solids.[17]

Table 4. Results of the adsorption experiments at CO_2 pressure of 1 bar and 20 bars.[4]

	CO_2 adsorption capacities (%)					
	25 °C		120/180 °C*		200 °C	
Adsorbent	20 bar	1 bar	20 bar	1 bar	20 bar	1 bar
AC1	3.30	0.75	**4.29**	**0.15**	4.70	0.55
AC2	2.66	0.53	**4.29**	**0.17**	4.58	0.35
AC3	2.30	0.39	**1.42**	**0.10**	3.39	0.11
AC4-200	20.19	7.70	8.54	1.43	4.16	0.43
AC4-250	22.74	8.87	13.19	2.51	4.59	0.35
AC4-300	19.49	7.24	10.55	1.84	2.57	0.15
AC5-175	17.08	7.07	6.79	1.14	2.61	0.38
AC5-200	17.80	7.26	7.97	1.82	3.40	0.36
AC5-250	13.57	5.38	9.07	2.12	4.92	0.58
AC5-250-400He	18.38	6.92	8.72	1.91	4.70	0.60
AC4-300-600He	20.82	7.06	9.82	1.59	4.44	0.89

(*) Data collected at 180 °C are shown in bold.

In order to analyze CO_2 adsorption kinetics on the adsorbents, kinetic plots of the samples involving the time to reach the equilibrium CO_2 uptake values at 1000 mbar were obtained at all temperature levels. Constant temperature and pressure were maintained during the equilibrium measurements. The kinetic plots [adsorbed amount of CO_2 (q_t) in mg/g versus time (t) in min] of AC4 samples are given for adsorption at

Table 5. Correlation coefficients obtained for the pseudo-first order kinetic, pseudo-second order kinetic, and intraparticle diffusion models.

Adsorbent	R^2								
	25 °C			120/180 °C			200 °C		
	1st order	2nd order	intra-par. diffn	1st order	2nd order	intra-par. diffn	1st order	2nd order	intra-par. diffn
AC1	**0.9945**	0.9810	0.9990	0.5787	0.0699	0.4770	0.7432	0.3027	0.8336
AC2	**0.9988**	0.9815	0.9915	0.9331	0.6058	0.9838	0.9286	0.7617	0.5121
AC3	**0.9978**	0.9882	0.9952	0.6943	0.2926	0.7207	0.3030	0.0001	0.1086
AC4-300	0.9871	**0.9990**	0.9991	**0.9869**	0.9484	0.9849	0.0131	0.0012	0.5939
AC4-200	0.9871	**0.9990**	0.9989	**0.9907**	0.9655	0.9806	**0.9905**	0.2869	0.9713
AC4-250	0.9823	**0.9990**	0.9984	**0.9930**	0.9301	0.9923	0.9086	0.7406	0.9665
AC5-175	0.9429	**0.9980**	0.9929	**0.9912**	0.7534	0.9698	0.9706	0.5337	0.9707
AC5-200	0.9378	**0.9990**	0.9911	**0.9921**	**0.9917**	0.9958	0.9260	0.7302	0.9688
AC5-250	**0.9927**	**0.9983**	0.9893	**0.9950**	**0.9938**	0.9986	**0.9915**	0.9042	0.9880
AC4-300-600He	**0.9981**	0.9331	0.9812	**0.9959**	0.9743	0.9908	0.9603	0.7043	0.6570
AC5-250-400He	**0.9965**	**0.9987**	0.9930	**0.9959**	0.9736	0.9900	0.9817	0.6407	0.7144

25 and 120 °C as an example in Figure 4. The CO_2 adsorption kinetic plots revealed a two-step adsorption process for all the activated carbon adsorbents, a relatively fast kinetic region phase followed by a slow one until reaching the equilibrium for all temperature levels, 25 °C, 120 °C, and 200 °C (not shown). The distinction between those two phases can be followed from the plot; the data sampling time close to the equilibrium is so small that those points form a solid curve. The pseudo-first and pseudo-second order kinetic models as well as the intraparticle diffusion model were applied to the kinetic data. Figures 5 and 6 show examples of experimental data fitted to linearized pseudo-first order and pseudo- second order kinetics models, respectively. It should be kept in mind that the data belonging to the linear kinetic regions of the q_t versus time (t) kinetic plots (Figure 4) were fitted to the models mentioned. The correlation coefficients (R^2) obtained are given in Table 5. The trendlines with R^2 values above 0.99 are accepted as valid and are indicated in bold. The parameters obtained from the application of pseudo-first and pseudo-second order kinetic models to the kinetic data yielding R^2 values higher than 0.99 are given in Tables 6 and 7, respectively. On the other hand, the parameters for the intraparticle diffusion model are not shown since model application did not yield physically meaningful parameters despite the good mathematical fit, suggesting intraparticle diffusion was not the rate limiting step in the CO_2 adsorption process on any of the adsorbents studied at any temperature level.

The comparison between the adsorbed amounts of CO_2 at equilibrium time (q_e) obtained from experiments and through calculation using kinetic expressions gives an idea about the suitability of the pseudo-first and pseudo-second order rate equations to the data range until reaching q_e for each adsorbent. It is quite clear both from Figure 4 having two adsorption phases and from the difference between the calculated and experimental q_e values given in Tables 6 and 7 for the pseudo-first and pseudo-second order kinetics, respectively, the kinetics of CO_2 adsorption should be regarded neither as pseudo-first order nor as pseudo-second order if the whole adsorption data range until reaching q_e is considered. On the other hand, the kinetic expression showing almost perfect fit to the experimental data points for the kinetic region and yielding relatively lower deviation from the experimental equilibrium adsorption may be safely considered more plausible. Thus at 25 °C the CO_2 adsorption mechanisms of the alkali impregnated AC4 and AC5 samples are not governed by the pseudo-first or pseudo-second order kinetic equations most probably due to the complex nature of the adsorbents. However, at 120 °C, the adsorption kinetics of those samples can be explained by the pseudo-first order kinetics. One can propose further that AC4 and AC5 samples become more stabilized at ca. 120 °C considering the fact that the

kinetic behavior of the more stable samples, such as the ones subjected to high temperature helium treatments and the nonimpregnated adsorbents, are well explained by the pseudo-first order kinetics at 25 °C.

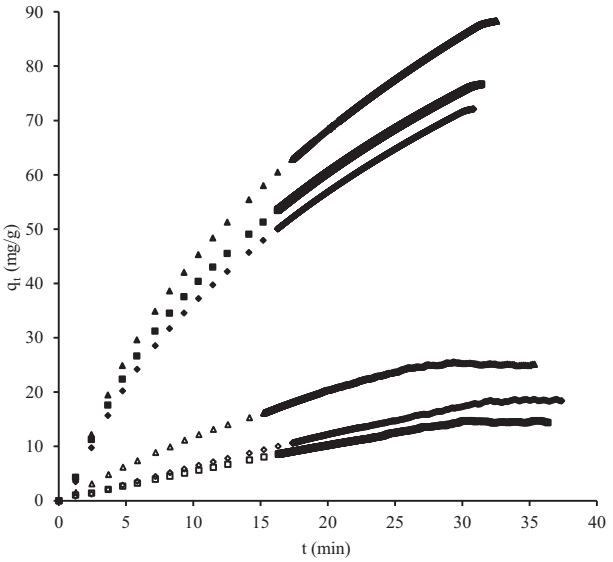

Figure 4. The kinetic plots of AC4 samples: (■) AC4-200, (▲) AC4-250, and (♦) AC4-300 at 25 °C (filled data points) and 120 °C (hollow data points).

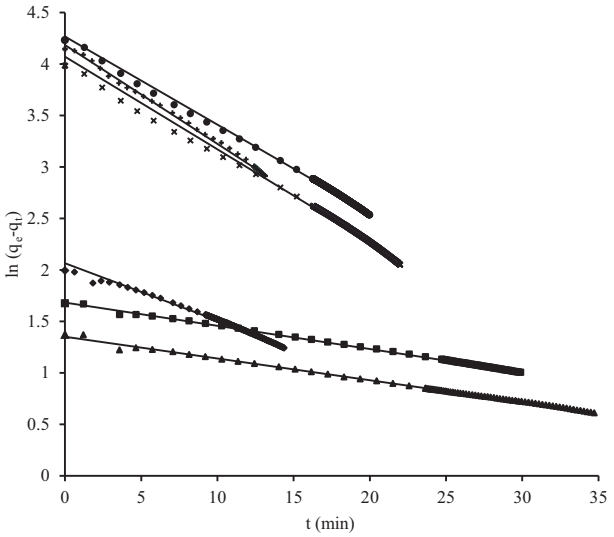

Figure 5. Pseudo-first order kinetic model for adsorption of CO_2 at 25 °C on (♦) AC1, (■) AC2, (▲) AC3, (×) AC5-250, (+) AC4-300-600He, and (●) AC5-250-400He.

3. Conclusion

The correlation parameters have shown that experimental isotherm data for the impregnated samples (AC4 and AC5) are in fair agreement with Langmuir and Freundlich model predictions, but the data are better described by the D-R equation. This indicates the possible complicated adsorption phenomena on activated carbon-based adsorbents prepared; competitive or multilayer CO_2 adsorption can occur in the micropores of the adsorbents. The results indicate that the micropore capacities obtained from the D-R model were consistent with the previously conducted characterization studies and the variance in the carbon surface chemistry. The CO_2 adsorption kinetic plots revealed a two-step adsorption process for all the activated carbon adsorbents: a relatively fast kinetic region phase followed by a slow one until reaching the equilibrium. Pseudo-first and pseudo-second order kinetics explain adsorption for the kinetic region for most of the samples. Intraparticle diffusion does not yield physically meaningful parameters. When the whole adsorption data range until reaching q_e is considered, the adsorption cannot be explained by any model due to the complex nature of the adsorbents, but the adsorption behavior fits rather well to pseudo-first order kinetics at 120 °C for the alkali impregnated samples, and at 25 °C for nonimpregnated samples and the adsorbents subjected to high temperature helium treatment as well.

4. Experimental

The chemically modified activated carbon-based adsorbents used in this study are given in Table 8. The details of the different pretreatment procedures applied to Norit ROX 0.8 samples, in crushed and sieved form (200–300 μm) are as follows: (i) Commercial AC was washed with 2 N HCl solution for 12 h and then washed with distilled water for 6 h under reflux. These were followed by overnight drying at 110 °C (AC1), (ii) AC1

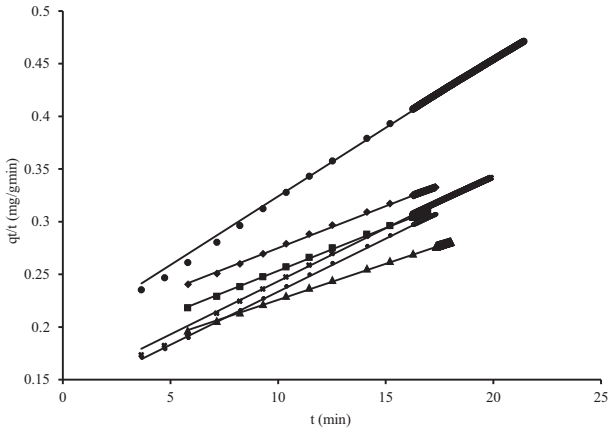

Figure 6. Pseudo-second order kinetic model for adsorption of CO_2 at 25 °C on (■) AC4-200, (▲) AC4-250, (♦) AC4-300, (×) AC5-175, (+) AC5-200, and (●) AC5-250.

Table 6. Pseudo-first order kinetic model parameters for the adsorption of CO_2 on AC samples.

Adsorbent	T (°C)	R^2	$k_1 \times 10^2$ (min^{-1})	q_e (plot) (mg/g)	q_e (exp) (mg/g)	error (%)
AC1	25	0.9945	5.83	8.127	7.347	10.62
AC2	25	0.9988	2.25	5.384	5.340	0.82
AC3	25	0.9978	2.11	3.863	3.925	1.58
AC4-200	120	0.9907	6.14	15.599	14.348	8.72
	200	0.9905	4.41	4.497	4.304	4.48
AC4-250	120	0.9930	7.35	26.902	25.104	7.16
AC4-300	120	0.9869	5.67	20.387	18.387	10.88
AC5-175	120	0.9912	6.72	12.862	11.325	13.57
AC5-200	120	0.9921	6.80	20.985	18.185	15.40
AC5-250	25	0.9927	9.00	58.674	53.759	9.14
	120	0.9950	6.85	23.042	21.188	8.75
	200	0.9915	6.21	6.167	5.737	7.50
AC4-300-600He	25	0.9981	9.59	65.687	63.203	3.93
	120	0.9959	7.76	16.446	15.578	5.57
AC5-250-400He	25	0.9965	8.56	71.322	68.903	3.51
	120	0.9959	6.44	20.557	19.058	7.87

Table 7. Pseudo-second order kinetic model parameters for the adsorption of CO_2 on AC samples.

Adsorbent	T (°C)	R^2	$k_2 \times 10^4$ (g mg^{-1} min^{-1})	q_e (plot) (mg/g)	q_e (exp) (mg/g)	error (%)
AC4-300	25	0.9990	3.28	125.000	72.099	73.37
AC4-200	25	0.9990	3.74	125.000	76.624	63.13
AC4-250	25	0.9990	2.29	166.667	88.307	88.74
AC5-175	25	0.9980	7.00	100.000	70.307	42.23
AC5-200	25	0.9990	7.58	100.000	84.431	18.44
	120	0.9917	5.59	40.984	18.185	125.37
AC5-250	25	0.9983	8.51	77.519	53.759	44.20
	120	0.9938	5.15	47.170	21.188	122.63
AC5-250-400He	25	0.9987	6.60	99.010	68.903	43.69

was oxidized in 5% O_2–95% N_2 mixture at 450 °C for 10 h (AC2), (iii) AC1 was oxidized in 5 N HNO_3 solution for 3 h and washed with boiling distilled water until the pH reached 5.5. These treatments were followed by overnight drying at 110 °C (AC3). The adsorbents having 10 wt.% Na_2CO_3 on AC2 and AC3 were prepared by incipient-to-wetness impregnation technique and are named AC4 and AC5, respectively. They were calcined at different temperatures in 5% O_2–95% N_2 mixture for 2 h after the impregnation procedure (Table 8). All adsorbents were used as such or were subjected to He treatment for 2 h at 400 °C or 600 °C.[4] The CO_2 adsorption capacities and CO_2 adsorption isotherms in the range of 0–20 bar were obtained by using an Intelligent Gravimetric Analyzer (Hiden Isochema). High purity CO_2 gas was connected directly to the analyzer. The adsorption and desorption isotherms of all samples were obtained at 25, 120/180, and 200 °C. In order to eliminate humidity and trapped gasses, 60–90 mg samples were outgassed at room temperature for 24 h prior to the adsorption runs. A detailed characterization study including BET (given in Table 9), SEM, and FTIR-DRIFTS studies was conducted on the adsorbent samples.[4] The analysis of the adsorption isotherms was carried out by means of the Langmuir, Freundlich, and D-R methods. Pseudo-first and pseudo-second order kinetic models as well as the intraparticle diffusion model were used to describe the kinetic behavior of the adsorbents.

Table 8. List of activated carbon-based adsorbents.

Name	Treatment
AC1	NORIT ROX washed with 2 N HCl
AC2	Air oxidized (in 5% O_2–95% N_2 mixture at 450 °C) AC1
AC3	Oxidized (in 5 N HNO_3) AC1
AC4-200	10% Na_2CO_3 impregnated and calcined in 5% O_2–95% N_2 mixture (200 °C) AC2
AC4-250	10% Na_2CO_3 impregnated and calcined in 5% O_2–95% N_2 mixture (250 °C) AC2
AC4-300	10% Na_2CO_3 impregnated and calcined in 5% O_2–95% N_2 mixture (300 °C) AC2
AC5-175	10% Na_2CO_3 impregnated and calcined in 5% O_2–95% N_2 mixture (175 °C) AC3
AC5-200	10% Na_2CO_3 impregnated and calcined in 5% O_2–95% N_2 mixture (200 °C) AC3
AC5-250	10% Na_2CO_3 impregnated and calcined in 5% O_2–95% N_2 mixture (250 °C) AC3
AC5-250-400He	AC5-250 subjected to He treatment at 400 °C for 2 h
AC4-300-600He	AC4-300 subjected to He treatment at 600 °C for 2 h

Table 9. BET surface areas of adsorbents.

Adsorbent	BET (m_2/g)
AC1	856
AC2	1228
AC3	667
AC4-200	687
AC4-250	579
AC4-300	771
AC5-175	564
AC5-200	888
AC5-250	1190

Acknowledgments

This work is financially supported by TÜBİTAK through project 113M263 and by Boğaziçi University Research Fund through project BAP-M6755.

References

1. Wilcox, J. *Carbon Capture*; Springer: New York, NY, USA, 2012.
2. Zhang, Z.; Xu, M.; Wang, H.; Li, Z. *Chem. Eng. J.* **2010**, *160*, 571-577.
3. Auta, M.; Amat Darbis, N. D.; Mohd Din, A. T.; Hameed, B. H. *Chem. Eng. J.* **2013**, *233*, 80-87.
4. Caglayan, B. S.; Aksoylu, A. E. *J. Hazard. Mater.* **2013**, *252-253*, 19-28.
5. Figueiredo, J. L.; Pereira, M. F. R.; Freitas, M. M. A.; Orfao, J. J. M. *Carbon* **1999**, *37*, 1379-1389.
6. Aksoylu, A. E.; Freitas, M. M. A.; Figueiredo, J. L. *Appl. Catal. A* **2000**, *192*, 29-42.
7. Plaza, M. G.; Pevida, C.; Arenillas, A.; Rrubiera, F.; Pis, J. J. *Fuel* **2007**, *86*, 2204-2212.
8. Shafeeyan, M. S.; Daud, W. M. A. W.; Houshmand, A.; Shamari, A. *J. Anal. Appl. Pyrolysis* **2010**, *89*, 143-151.
9. Biniac, S.; Szymanski, G.; Siedlewski, J.; Swiatkowski, A. *Carbon* **1997**, *35*, 1799-1810.
10. Dastgheib, S. A.; Karanfil, T.; Cheng, W. *Carbon* **2004**, *42*, 547-557.
11. Chen, W.; Cannon, F. S.; Rangel-Mendez, J. R. *Carbon* **2005**, *43*, 573-580.
12. Tan, Y. L.; Azharul Islam, M.; Asif, M.; Hameed, B. H. *Energy* **2014**, *77*, 926-931.
13. Lillo-Rodenas, M. A.; Cazorla-Amoros, D.; Linares-Solano, A. *Carbon* **2003** *41*, 267-275.
14. Yong, Z.; Mata, V.; Rodrigues, A. E. *Adsorption* **2001** *7*, 41-50.
15. Somy, A.; Mehrnia, M. R.; Amrei, H. D.; Ghanizadeh, A.; Safari, M. *Int. J. Greenhouse Gas Control* **2009**, *3*, 249-254.
16. Song, H. K.; Lee, K. H. *Sep. Sci. Technol.* **1998**, *33*, 2039-2057.
17. Gil, A.; Grange, P. *Colloid Surf. A* **1996**, *113*, 39-50.
18. Daley, M. A.; Tandon, D.; Economy, J.; Hippo, E. J. *Carbon* **1996**, *34*, 1196-1200.
19. Carrott, P. J. M.; Ribeiro Carrott, M. M. L.; Suhas. *Carbon* **2010**, *48*, 4162-4168.
20. Mourao, P. A. M.; Carrott, P. J. M.; Ribeiro Carrott, M. M. L. *Carbon* **2006**, *44*, 2422-2429.
21. Nguyen, C.; Do, D. D. *Carbon* **2001**, *39*, 1327-1336.
22. Ushiki, I.; Ota, M.; Sato, Y.; Inomata, H. *Fluid Phase Equilib.* **2013**, *344*, 101-107.
23. Yan, X.; Komarneni, S.; Yan, Z. *J. Colloid Interface Sci.* **2013**, *390*, 217-224.
24. Burevski, D. *Colloid Polym. Sci.* **1982**, *260*, 623-627.
25. Caglayan, B. S.; Soykal, I. I.; Aksoylu, A. E. *Appl. Catal. B* **2011**, *106*, 540-549.
26. Shafeeyan, M. S.; Daud, W. M. A. W.; Shamiri, A. *Chem. Eng. Res. Des.* **2014**, *92*, 961-988.
27. Dantas, T. L. P; Luna, F. M. T.; Silva Jr., I. J.; de Azevedo, D. C. S.; Grande, C. A.; Rodrigues, A. E.; Moreira, R. F. P. M. *Chem. Eng. J.* **2011**, *169*, 11-19.
28. Tran, C. D.; Duri, S.; Delnri, A.; Franco, M. *J. Hazard. Mater.* **2013**, *252-253*, 355-366.
29. Borah, D.; Satokawa, S.; Kato, S.; Kojima, T. *J. Hazard. Mater.* **2009**, *162*, 1269-1277.
30. Pulido Melian, E.; Gonzalez Diaz, O.; Arana, J.; Dona Rodriguez, J. M.; Tello Rendon, E.; Herrera Melian, J. A. *Catal. Today* **2007**, *129*, 256-262.
31. Yu, L.; Luo, Y. *J. Environ. Chem. Eng.* **2014**, *2*, 220-229.
32. Ho, Y. S.; McKay, G. *Process Biochem.* **1999**, *34*, 451-465.

33. Cheung, O.; Bacsik, Z.; Liu, Q.; Mace, A.; Hedin, N. *Appl. Energy* **2013**, *112*, 1326-1336.
34. Ruthven, D. M. *Microporous Mesoporous Mater.* **2012**, *162*, 69-79.
35. Ma, Z. H.; Li, Q.; Yue, Q. Y.; Gao, B. Y.; Li, W. H.; Xu, X. *Chem. Eng. J.* **2011**, *171*, 1209-1217.
36. Shi, M.; Wang, Z.; Zheng, Z. *J. Environ. Sci.* **2013**, *25*, 1501-1510.
37. Kilduff, J. E.; King, C. J. *Ind. Eng. Chem. Res.* **1997**, *36*, 1603-1613.